

# Screening and Identification of Metabolites from Sambiloto (*Andrographis paniculata*) Ethanol Extract for Pro-Inflammatory Cytokines Inhibitory through *In Silico* and *In Vitro* Approaches

Evul Winoto Lukito<sup>1</sup>, Dyah Iswanti<sup>1,2\*</sup>, Budhi Antariksa<sup>3</sup>, Mohamad Rafi<sup>1,2</sup>, Setyanto Tri Wahyudi<sup>2,4</sup>

Evul Winoto Lukito<sup>1</sup>, Dyah Iswanti<sup>1,2\*</sup>, Budhi Antariksa<sup>3</sup>, Mohamad Rafi<sup>1,2</sup>, Setyanto Tri Wahyudi<sup>2,4</sup>

<sup>1</sup>Department of Chemistry, Faculty of Mathematics and Natural Sciences, IPB University, Bogor 16680, INDONESIA.

<sup>2</sup>Tropical Biopharmaca Research Center, IPB University, Bogor 16128, INDONESIA.

<sup>3</sup>Department of Pulmonology and Respiratory Medicine, Faculty of Medicine, Universitas Indonesia, Persahabatan Hospital, INDONESIA.

<sup>4</sup>Department of Physics, Faculty of Mathematics and Natural Sciences, IPB University, Bogor 16680, INDONESIA.

## Correspondence

Dyah Iswanti

Department of Chemistry, Faculty of Mathematics and Natural Sciences & Tropical Biopharmaca Research Center, IPB University, Bogor 16128, INDONESIA.

E-mail: dyahis@apps.ipb.ac.id

## History

- Submission Date: 08-11-2023;
- Review completed: 16-12-2023;
- Accepted Date: 26-12-2023.

DOI : 10.5530/pj.2024.16.18

Article Available online

<http://www.phcogj.com/v16/i1>

## Copyright

© 2024 Phcogj.Com. This is an open-access article distributed under the terms of the Creative Commons Attribution 4.0 International license.

## ABSTRACT

**Objective:** *Andrographis paniculata* has long been a traditional medicinal plant in Indonesia. This study is intended to evaluate the anti-pro-inflammatory cytokines of 98% ethanol extract of *A. paniculata* by *in vitro* and *in silico* approaches. Inhibition of pro-inflammatory cytokines is also one of the therapies in treating COVID-19. **Methods:** The molecular docking approach was utilized as a first screening to evaluate the potential for suppression of macrophage cell activation; an ADMET prediction test was performed to determine the pharmacological, pharmacokinetic, and toxicity as a therapeutic target. TNF- $\alpha$ , IL-1 $\beta$ , and IL-6 levels were measured using an ELISA method to investigate anti-cytokine pro-inflammatory activity in LPS-induced RAW 264.7 macrophage cells. LC-MS/MS was used to identify additional metabolite compounds. **Results:** Ethanol extract containing particular metabolites 14-Deoxyandrographoside and 14-Deoxy-17-hydroxyandrographolide inhibited TNF- $\alpha$  and IL-1 $\beta$  by 100% and IL-6 by 85.59%, respectively. While compared to the Dexamethasone molecule as a positive control, preliminary screening and ADMET prediction for the metabolite compound 14-Deoxyandrographoside exhibited relatively high binding stability to the CD14 receptor by -7.5 kcal/mol and was safe against various ADMET indications. **Conclusions:** This study reveals that the compound 14-Deoxyandrographoside in pure ethanol extract is a potential anti-cytokine agent candidate for treating pro-inflammatory cytokines, including COVID-19 infection.

**Keywords:** LC-MS/MS, Molecular docking, Pro-inflammatory cytokines, Sambiloto.

## INTRODUCTION

Severe Acute Respiratory Syndrome Coronavirus-2 (SARS-CoV-2) is a coronavirus that causes severe acute respiratory syndrome known as Coronavirus Disease 2019.<sup>1</sup> Acute respiratory distress syndrome (ARDS) is the leading cause of death in COVID-19 patients.<sup>2,3</sup> The cause of ARDS in COVID-19 infection is the occurrence of a cytokine storm.<sup>4</sup> Cytokine storm is an event of excessive release of pro-inflammatory cytokines due to an uncontrolled systemic inflammatory response.<sup>5</sup> Sustained cytokine storm causes tissue damage, increasing the risk of vascular hyperpermeability, multiorgan failure, and death.<sup>6</sup> Inhibition of the pro-inflammatory cytokine storm in the early stages of COVID-19 is an effective therapeutic strategy to prevent the development of more severe ARDS.<sup>7</sup> Since WHO has not yet recommended particular medications for the treatment of COVID-19, the focus of current COVID-19 therapy is on anti-cytokines or immunomodulators.<sup>8,9</sup> Finding a source for plant metabolite molecules with anti-cytokine properties is an essential challenge. *In silico* analysis is the most widely used method as an initial screening to find and analyze potential candidates for plant metabolite compounds that have the potential as pro-inflammatory anti-cytokines for COVID-19 therapy. *In silico* analysis of several plants shows promising potential as a target for COVID-19 therapy. *A. paniculata* is one of the plants reported to have inhibit SARS-CoV-2.<sup>10-12</sup> *A. paniculata* is reported to have metabolite compounds with

a pharmacological activity that can reduce the characteristics of the pathogenesis of COVID-19, such as anti-inflammatory,<sup>13</sup> immunomodulator,<sup>7</sup> and antiviral.<sup>10-12</sup>

*A. paniculata* is a plant that grows well in Indonesia and has been widely used to treat COVID-19 in several Asian countries.<sup>14,15</sup> The primary metabolites of *A. paniculata* are andrographolide, neoandrographolide, 14-deoxyandrographolide, and 14-deoxy-11,12-didehydroandrographolide.<sup>13</sup> Many studies have been carried out on *A. paniculata* as an anti-inflammatory. However, screening for the potential of inhibiting *A. paniculata* metabolites against the production of pro-inflammatory cytokines has not been widely reported. Hence, screening and characterization of metabolites of *A. paniculata*, which have the potential as anti-cytokines, need to be carried out.

Currently, the screening method for metabolites of medicinal plants by binding them to target cells is widely used because it is more effective and efficient.<sup>16-18</sup> Macrophages are the main cells in the immune system that regulate the body's defense mechanism against disease.<sup>8</sup> Microorganism infection through the CD14 receptor will activate macrophage cells to release several inflammatory mediators, including pro-inflammatory cytokines.<sup>19</sup> In this study, the molecular docking method of *A. paniculata* metabolites against the structure of the CD14 protein was used as an initial screening to determine the potential for inhibiting macrophage cell activation based on its affinity energy value. The ADMET prediction analysis carried out the

**Cite this article:** Lukito EW, Iswanti D, Antariksa B, Rafi M, Wahyudi ST. Screening and Identification of Metabolites from Sambiloto (*Andrographis paniculata*) Ethanol Extract for Pro-Inflammatory Cytokines Inhibitory through *In Silico* and *In Vitro* Approaches. Pharmacogn J. 2024;16(1): 131-140.

metabolite compound with the best affinity energy to determine its inhibitory potential based on pharmacology, pharmacokinetics, and toxicity as a target for COVID-19 therapy. The *in vitro* analysis was carried out by binding the metabolite compound *A. paniculata* to RAW 264.7 macrophage cells induced by LPS to determine the bioactivity of inhibiting the production of pro-inflammatory cytokines, namely IL-6, IL-1 $\beta$ , and TNF- $\alpha$ . The metabolites of ethanol extract of *A. paniculata* were identified using UHPLC-Q-Orbitrap HRMS.<sup>20,21</sup>

## MATERIALS AND METHODS

### Molecular Docking

#### Protein Preparation

The crystal structure of the CD14 protein or macrophage cell receptor (PDB ID: 4GLP) was downloaded from the RCSB Protein Data Bank (<https://www.rcsb.org/>), and then optimization, minimization, and checking of missing residues were carried out using AMBER20.

#### Protein Preparation

A total of 35 structures of *A. paniculata* metabolite compounds and Dexamethasone compounds as positive controls were downloaded from PubChem (<https://pubchem.ncbi.nlm.nih.gov/>), then the collected ligands were optimized using ORCA.<sup>22</sup>

### Molecular Docking Simulation

Molecular docking simulations investigated the interaction between *A. paniculata* metabolites and Dexamethasone with the CD14 receptor protein (4GLP). Dexamethasone is a synthetic glucocorticoid with anti-inflammatory and immunosuppressive properties that is used to treat a variety of disorders.<sup>23–26</sup> We optimized the structure of the *A. paniculata* metabolite in the previous step. Blind docking was performed to discover the active site of CD14 macrophages and then targeted docking was employed using virtual screening to determine the position with the greatest affinity energy. The coordinates  $x = 51.795$ ;  $y = 35.218$ ; and  $z = 2.484$  were utilized in the simulation using Autodock-Vina with five repetitions. The assembly docking step will further process the five highest compounds that emerge consistently in five repetitions.

### Ensemble Docking Structures Using Molecular Dynamics Simulation

In this study, molecular dynamics simulations were carried out to create a docking ensemble structure. The AMBER ff14sb force field is used to model the structure of the 4GLP protein.<sup>27</sup> The protein files were put into a 20 $\times$ 20 $\times$ 20 Å solvent box. To prepare the simulation system, tleap software was used.

#### a) Minimization Step

The simulation begins with energy minimization. The phase aims to reduce the energy required for the complex structure to adapt to its natural state while avoiding undesirable van der Waals interactions. Energy minimization was carried out in stages with different restraints at each stage: 1000, 500, 250, 100, and 50 kcal/mol.

#### b) Heating and Equilibration Step

When the minimization stage is finished, the confinement is eliminated and the molecules are free for movement. The heating, equilibration, and molecular dynamics simulations were then performed. The Langevin protocol was used in the warm-up stage, along with the NVT dynamic ensemble. The system was heated to 300 K while maintaining a 10 kcal/mol confinement. The purpose of this constraint is to maintain the protein structure molecules stable during heating. Following that, an equilibrium stage is performed in which the limitations are progressively lifted and the system adapts to a certain temperature.

#### c) Molecular Dynamics Simulation and Ensemble Docking

The step is continued using 200 ns molecular dynamics simulations to generate 10 clusters for use in the assembly docking stage. The docking process was carried out by considering the interaction between the compounds and the 4GLP protein. After the docking procedure is completed, the docking findings are analyzed and ranked based on the affinity score or bond energy between the molecule and the target protein. Compounds with high affinity or bond energy scores will be chosen for the molecular dynamics modeling of protein complexes. This step aims to discover more about the stability and dynamics of the interactions between these chemicals and the target protein. As a result, the assembly docking step is expected to offer more information about the possible interactions between the tested drugs and the 4GLP target protein.

### Complex Structure Molecular Dynamics Simulation

The molecular dynamics of the ligand, 4GLP protein, and ligand-macromolecule complex in water were simulated in the final stage. The same folder contains pre-processed.pdb macromolecule and .mol2 ligand files. The ligand structures were loaded using the Antechamber software and the results were stored in .mol2 files. The .mol2 files were then used to generate the .frcmd file using the parmchk command. The topology and coordinates were generated using the tLeap program and the leap.in file. Minimization, heating, equilibration, and molecular dynamics simulations were performed on the 4GLP protein-ligand complex.

#### a) Complex Structure Analysis

The RMSD (Root Mean Square Deviation) technique compared molecular structural changes during simulation to the starting structure. RMSD provides information about the stability and convergence of the simulation.<sup>28</sup>

#### Prediction of Absorption Distribution Metabolism Excretion Toxicology (ADMET)

Metabolite compounds that show stable affinity energy in ensemble docking simulations, followed by ADMET properties analysis. ADMET predictions were performed using the Admet SAR 2.0 online server (<http://lmmd.ecust.edu.cn/admetSar2/>).

### Preparation and Sample Extraction

Extraction was carried out by the maceration method. *A. paniculata* leaf samples were cleaned by washing with water. The samples were dried in the sun and then crushed into 80-mesh powder. Approximately 25 g of the powder was added with 250 mL of 98% ethanol, then immersed with continuous stirring for 6 hours, then the sample was left for 12 hours without stirring. The extraction was repeated five times, and the filtrate was collected and concentrated using a rotary evaporator at 40 °C. The extract was then stored in a freezer at -80 °C.<sup>29</sup>

### Pro-inflammatory Cytokines Inhibitory Assay

#### RAW 264.7 Macrophage Cell Culture

RAW 264.7 macrophage cells were obtained from the Primate Research Center, IPB University, Bogor, Indonesia. Cells were grown in DMEM medium with 10% FBS and 1% penicillin-streptomycin. Cells were incubated at 37 °C with 5% CO<sub>2</sub> humidity until cells were confluent, then cells were harvested with trypsin-EDTA.<sup>30</sup>

#### Cell Viability Test

The cell viability test was carried out using the MTT method.<sup>31</sup> 1  $\times$  10<sup>4</sup> cells per well RAW 264.7 cells were planted in 96-well plates and then incubated for 24 hours. The discarded medium was replaced with a new

medium and added to the test sample at various concentrations of 5, 25, 50, and 100 µg/mL, then incubated again for 24 hours. The medium was removed, then the cells were washed with PBS. 10 µL of 5 mg/mL MTT solution was added to each well and again incubated for 4 hours. The formed formazan crystals were dissolved in 100 µL DMSO. Absorbance was measured using a microplate reader at a wavelength of 570 nm.

### Pro-Inflammatory Cytokine Inhibitory Assay

Cytokine inhibitory activity was carried out by measuring TNF- $\alpha$ , IL-1 $\beta$ , and IL-6 levels in LPS-stimulated RAW 264.7 cells using the ELISA method. RAW 264.7 cells of  $1 \times 10^3$  cells per well were planted in 96 well plates and then incubated for 24 hours. The medium was discarded, replaced with a new medium, and added to the test sample at 20 µg/mL, 30 µg/mL, and 40 µg/mL. The cells were incubated again for 2 hours, then the cells were stimulated with 1 µg/mL LPS and incubated again for 24 hours. The medium was taken and then centrifuged at 2000 rpm for 10 minutes. The supernatant was collected for measurement of TNF- $\alpha$ , IL-1 $\beta$ , and IL-6 levels using the Elabscience Mouse Elisa kit according to the instructions for use.

### Identification of Metabolite Compounds of *A. paniculata* Ethanol Extract

#### Sample Solution Preparation

As much as 5 mg of the ethanol extract of *A. paniculata* leaves was dissolved in 1 mL of LC-MS grade methanol, followed by sonication for 30 minutes. The sample solution was filtered with a 0.22 µm filter membrane. The filtrate was analyzed using UHPLC-Q-Orbitrap HRMS to separate and identify metabolites.

#### LC-MS/MS Analysis

The metabolites of the ethanol extract of *A. paniculata* leaves were separated using a Vanquish Flex UHPLC-Q Exactive Plus Orbitrap-High Resolution Mass Spectrometer with Accucore C18 (100  $\times$  2.1 mm, 1.5 m) as a column. The mobile phase consisted of 0.1% formic acid in water (A) and 0.1% formic acid in acetonitrile (B). The gradient elution is formatted as follows: 15% (B) from 0 to 1 min, 15-55% (B) from 1 to 20 min, 55-95% (B) from 20 to 23 min, 95% (B) from 23 to 28 minutes, then 15% (B) from 28 to 30 minutes. The flow rate used was 0.2 mL/minute with an injection volume of 2.0 µL. The ionization source used in the MS system is ESI, with positive and negative ionization modes in the m/z range of 100-1500. The capillary temperature used was 320 °C, the spray voltage was 3.8 kV, the casing gas and auxiliary gas flow rates were 15 and 3 mL/min, the automatic gain control (AGC) was  $3 \times 10^6$  and the injection time was set to 100 ms. The collision energies used are 18, 35, and 53 eV. The scan type used is full MS/dd MS2 and full scan data set with a resolving power of 70,000 FWHM.

### Data Analysis

Data obtained from UHPLC-Q-Orbitrap HRMS were processed using Compound Discoverer 2.2 with an in-house database collected from information on metabolites in *A. paniculata*. Identification of metabolites through several stages, namely the stage of selecting the appropriate spectrum, equalizing the retention time, detecting unknown compounds, grouping unknown compounds, predicting processes, searching mass lists, finding gaps for missing peaks, filtering compounds on blanks, and performing MS2 confirmation on identified metabolites.

## RESULTS AND DISCUSSION

### Molecular Docking Analysis

Molecular docking analysis is a quick approach for screening drugs based on the highest bond affinity energy ( $\Delta G$ ).<sup>32</sup> Molecular docking

data revealed that various *A. paniculata* metabolites had lower  $\Delta G$  than Dexamethasone, the positive control. A lower  $\Delta G$  value suggests that the ligand and protein are more stable.<sup>33</sup> The lower the  $\Delta G$ , the more spontaneous the bond between the ligand and the receptor.<sup>34</sup> Factors such as the number of hydrogen bonds, amino acid residues, and bond affinity energies influence the  $\Delta G$  of the receptor-ligand. The compounds with the lowest and most constant  $\Delta G$  values include beta-sitosterol, andrographiside, neoandrographolide, andrografolactone, skullcapflavone I, 14-Deoxyandrographoside, and apigenin. The seven best compounds were selected from 35 metabolites of *A. paniculata* for ensemble docking (Table 1).

### Ensemble Docking Analysis

Ensemble Docking is an advanced stage of molecular docking that is performed on ligands that have consistent affinity energy after five repetitions. The compounds Beta Sitosterol, Andrographiside, Neoandrographolide, Andrografolactone, Skullcapflavone I, 14-Deoxyandrographoside, and Apigenin were selected to perform the ensemble docking test on the structure of the CD14 receptor.

The assembly docking data is the average value of  $\Delta G$  from 10 different structural conformations of the receptor-ligand complex taken every 20 ns over a total span of 200 ns divided into 10 clusters (Table 2). The test results showed that the andrographiside, 14-deoxyandrographoside, neoandrographolide, and apigenin compounds had the lowest  $\Delta G$  value, which was less than -6.25 kcal/mol, this condition indicated that the four compounds had fairly good binding stability to the CD14 receptor.<sup>33</sup> Andrographiside, 14-Deoxyandrographoside, neoandrographolide, and apigenin were selected for further ADMET properties assay.

### ADMET Predictions

The ADMET (Absorption, Distribution, Metabolism, Excretion, and Toxicity) prediction was carried out for andrographiside, 14-Deoxyandrographoside, apigenin, and neoandrographolide so that information about the potential of these compounds to be developed as inhibitors based on their pharmacology, pharmacokinetics, and toxicity can be obtained.

The ADMET indicator is essential in the study of the development of drug compounds.<sup>35</sup> The five ADMET indicators used are Applicability Domain, Human Intestinal Absorption, AMES, Carcinogenicity, and Human Ether-a-go-go-Related Gene inhibition. Applicability domain test metabolites' physicochemical and topological properties, including molecular weight, alogP, number of atoms, number of aromatic rings, and number of hydrogen bond donors and acceptors. Human Intestinal Absorption shows the ability of metabolites to be absorbed into the intestine and digestive system. AMES Mutagenesis is the ability of metabolites to cause mutations and toxicity. Carcinogenicity indicates the potential of a compound to cause cancer. Human Ether-a-go-go-Related Gene inhibition is an inhibitory potential that causes fatal cardiac arrhythmias.<sup>35,36</sup>

The results of the ADMET prediction analysis are shown in Table 3. Positive and negative signs indicate that it can or cannot occur and decimal values 0 to 1 indicate the percentage of possibility or impossibility of occurring<sup>35,36</sup>. Based on the results in Table 3, apigenin, which has good enough ADMET testing results to be developed as a pro-inflammatory cytokine inhibitor, while andrographiside, 14-Deoxyandrographoside, and neoandrographolide compounds showed positive signs on the Human Ether-a-go-go-Related indicator. Gene inhibition was 67.6% and 75.9%, respectively. This condition is a potential inhibitor that can cause fatal cardiac arrhythmias.<sup>35</sup>

The findings of the molecular dynamics simulation demonstrate that the CD-14 receptor has an increase in RMSD values in the 0-10 ns

**Table 1: Value of Gibbs free energy ( $\Delta G$ ) of *A. paniculata* metabolites and positive control of CD14 macrophage receptors (PDB ID: 4GLP).**

No.	Ligand	$\Delta G$ (kcal/mol) replications:					$\Delta G$ average	SD
		1	2	3	4	5		
1	Beta Sitosterol	-8.4	-8.4	-8.7	-8.4	-8.5	-8.48	0.13
2	Andrographiside	-8.1	-8.1	-8.0	-8.1	-8.1	-8.08	0.04
3	Neoandrographolide	-7.5	-7.9	-7.8	-7.5	-7.9	-7.72	0.20
4	Andrografolaktan	-7.7	-7.6	-7.6	-7.7	-7.6	-7.64	0.05
5	Skullcapflavone I	-7.9	-7.4	-7.4	-7.9	-7.4	-7.60	0.27
6	14-Deoxyandrographoside	-7.5	-7.5	-7.4	-7.6	-7.5	-7.50	0.07
7	Apigenin	-7.6	-7.4	-7.6	-7.5	-7.4	-7.50	0.10
8	Andrografidin E	-7.5	-7.4	-7.4	-7.5	-7.4	-7.44	0.05
9	Dexamethasone (Positive control )	-7.5	-7.4	-7.4	-7.5	-7.4	-7.44	0.05
10	Luteolin	-7.6	-7.3	-7.3	-7.6	-7.3	-7.42	0.16
11	Wogonin	-7.7	-7.2	-7.2	-7.7	-7.2	-7.40	0.27
12	Bisandrographolide A	-7.0	-7.0	-7.6	-7.0	-8.1	-7.34	0.50
13	7-O-metilwogonin	-7.8	-7.0	-7.0	-7.8	-7.0	-7.32	0.44
14	Andrografidin A	-7.4	-7.1	-7.3	-7.4	-7.1	-7.26	0.15
15	Andrografidin C	-7.4	-7.1	-7.1	-7.4	-7.1	-7.22	0.16
16	Deoxyandrographolide	-7.3	-7.0	-7.0	-7.3	-6.9	-7.10	0.19
17	Andrographolide	-7.2	-7.0	-7.0	-7.2	-7.0	-7.08	0.11
18	Dehydroandrographoline	-7.1	-7.0	-7.1	-7.1	-7.1	-7.08	0.04
19	Isoandrographolide	-7.1	-7.0	-7.1	-7.1	-7.0	-7.06	0.05
20	3.14-Dideoxyandrographolide	-7.1	-7.0	-7.0	-7.1	-7.0	-7.04	0.05
21	14-Deoxy-11.12-didehydroandrographolide	-6.5	-7.1	-7.2	-7.1	-7.3	-7.04	0.31
22	3.4-Dicaffeoylquinic Acid	-7.0	-6.9	-7.0	-7.0	-7.2	-7.02	0.11
23	Andrograpanin	-7.1	-7.0	-6.9	-7.1	-7.0	-7.02	0.08
24	14-Deoxy-11-oxo-andrographolide	-7.2	-6.8	-6.9	-7.2	-6.8	-6.98	0.20
25	Diterpene II (Lactone)	-7.0	-7.1	-6.9	-7.0	-6.9	-6.98	0.08
26	5-Hydroxy-7.8.2-trimethoxyflavone-5-glucoside	-6.9	-6.9	-6.9	-6.9	-6.9	-6.90	0.00
27	14-Deoxyandrographolide	-6.9	-6.8	-6.8	-6.9	-6.9	-6.86	0.05
28	14-Deoxy-12-Hydroxyandrographolide	-7.0	-6.6	-6.6	-7.0	-6.6	-6.76	0.22
29	14-Deoxy-11-hydroxyandrographolide	-6.9	-6.6	-6.6	-6.9	-6.7	-6.74	0.15
30	1.8-dihydroxy-2.6-dimethoxyxanthan-9-one	-6.7	-6.5	-6.5	-6.7	-6.5	-6.58	0.11
31	Paniculide-A	-6.6	-6.3	-6.2	-6.6	-6.3	-6.40	0.19
32	5-Hydroxy-7.8.2'.3'-tetramethoxyflavone	-6.3	-6.5	-6.3	-6.3	-6.5	-6.38	0.11
33	Paniculide-C	-6.4	-6.4	-6.3	-6.4	-6.3	-6.36	0.05
34	Paniculide-B	-6.2	-6.2	-6.2	-6.2	-6.1	-6.18	0.04
35	Eugenol	-5.2	-5.0	-5.0	-5.2	-5.1	-5.10	0.10

**Table 2: Ensemble docking results of *A. paniculata* metabolites against CD14 macrophage receptors (PDB ID: 4GLP).**

Ligand	$\Delta G$ (kcal/mol) at measurement time (ns)										$\Delta G$ average	SD
	20	40	60	80	100	120	140	160	180	200		
Andrographiside	-6.4	-7.0	-6.8	-7.5	-7.8	-7.4	-5.9	-5.9	-6.3	-3.9	-6.49	1.12
14-Deoxyandrographoside	-6.5	-6.9	-6.4	-7.5	-7.2	-7.2	-5.7	-5.9	-6.1	-4.1	-6.35	0.99
Neoandrographolide	-6.9	-7.0	-7.0	-7.5	-7.5	-6.9	-5.8	-5.3	-5.5	-3.9	-6.33	1.17
Apigenin	-6.3	-6.8	-6.9	-6.8	-6.8	-7.2	-6.3	-5.8	-5.4	-4.1	-6.24	0.93
Skullcapflavone I	-6.4	-6.4	-6.8	-6.9	-6.9	-6.4	-5.7	-4.8	-5.3	-4.3	-5.99	0.92
Andrografolaktan	-6.5	-6.4	-6.6	-6.7	-6.4	-6.1	-6.0	-5.4	-5.6	-4.1	-5.98	0.79
Beta Sitosterol	-6.0	-6.8	-6.3	-7.3	-7.2	-5.9	-6.2	-5.0	-4.7	-3.3	-5.87	1.23

**Table 3: ADMET prediction of *A. paniculata* metabolites with the best  $\Delta G$  value using the ADMET SAR 2.0 online server.**

ADMET indicator	<i>A. paniculata</i> metabolite compounds			
	Andrographiside	14-Deoxyandrographoside	Neoandrographolide	Apigenin
Applicability Domain	In Domain	In Domain	In Domain	In Domain
Human Intestinal Absorption	(+) 0.8124	(+) 0.8124	(+) 0.8124	(+) 0.9881
AMES Mutagenesis	(-) 0.61	(-) 0.71	(-) 0.67	(-) 0.6741
Carcinogenicity	(-) 1	(-) 0.6266	(-) 1	(-) 1
Human Ether-a-go-go-Related Gene inhibition	(+) 0.6759	(+) 0.6759	(+) 0.7587	(-) 0.897

region, but beyond that period, the receptor has steady fluctuations and is in the 3.5 Å range. This indicates that the interaction between the ligand and the receptor occurs in a stable system for 100 ns. Meanwhile, RMSD ligand 20 varied at 100 ns but remained near the CD-14 receptor (<0.7 Å). Figure 1 illustrates the changes in the RMSD of the ligand and receptor during the simulation.

The results of the MMPBSA analysis showed that the CD-14 and apigenin receptors had a total MMPBSA energy of -8.3369 kcal/mol. MMPBSA energy is dominated by electrostatic interactions between CD-14 receptors and apigenin. The negative MMPBSA energy value indicates stable interaction between the CD-14 receptor and apigenin. These results may provide a further understanding of the strength of the bond between the ligand and the receptor and the interactions of the amino acid residues involved in the ligand-receptor complex.<sup>32</sup>

### Viability Test

The cell viability test was carried out using the MTT method to see the number of living cells after being given the extract, thereby knowing the concentration of the extract which is not toxic to RAW 264.7 cells. The results of the viability test showed a decrease in the number of living cells along with an increase in the concentration of the extract given (Figure 2). Test concentrations with a percentage of cell viability of less than 80% are test concentrations that are toxic to cells.<sup>37</sup> At a test concentration of 100 µg/mL, it causes up to 57% cell death, so the percent cell viability is 43%.

To determine the maximum test concentration with a viability of 100%, it was calculated using the linear equation of pure ethanol extract  $y = -0.802x + 131.84$  to obtain an antilog x value of 40 µg/mL. Then this dose was used to test the inhibitory activity of pro-inflammatory cytokines.

### Pro-Inflammatory Cytokine Inhibitory Activity

The inhibitory activity of pro-inflammatory cytokines was determined by measuring TNF-α, IL-1β, and IL-6 levels in LPS-stimulated RAW 264.7 cells using the ELISA method. The test results in Table 5 show that

**Table 4. Energy value of MMPBSA complex compound CD-14 and apigenin.**

Energy Component	E (kcal/mol)
Van der Waals	-8.23
EEL	-11.23
EPB	12.31
ENPolar	-1.13
Delta Gas	-19.52
Delta solv	11.18
TOTAL	-8.34

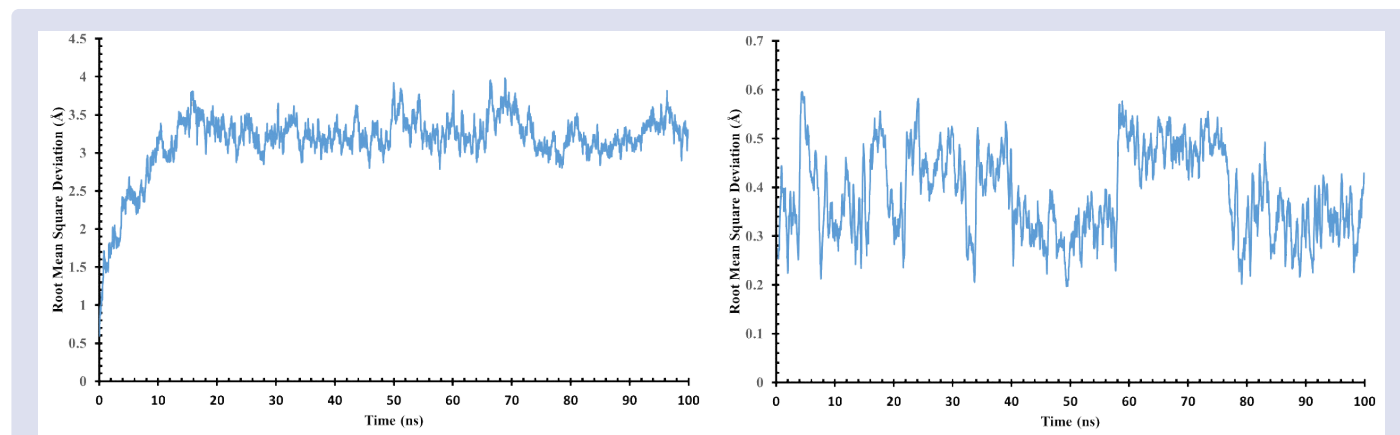


**Figure 1:** RMSD receptor CD-14 (a) and apigenin (b) values.

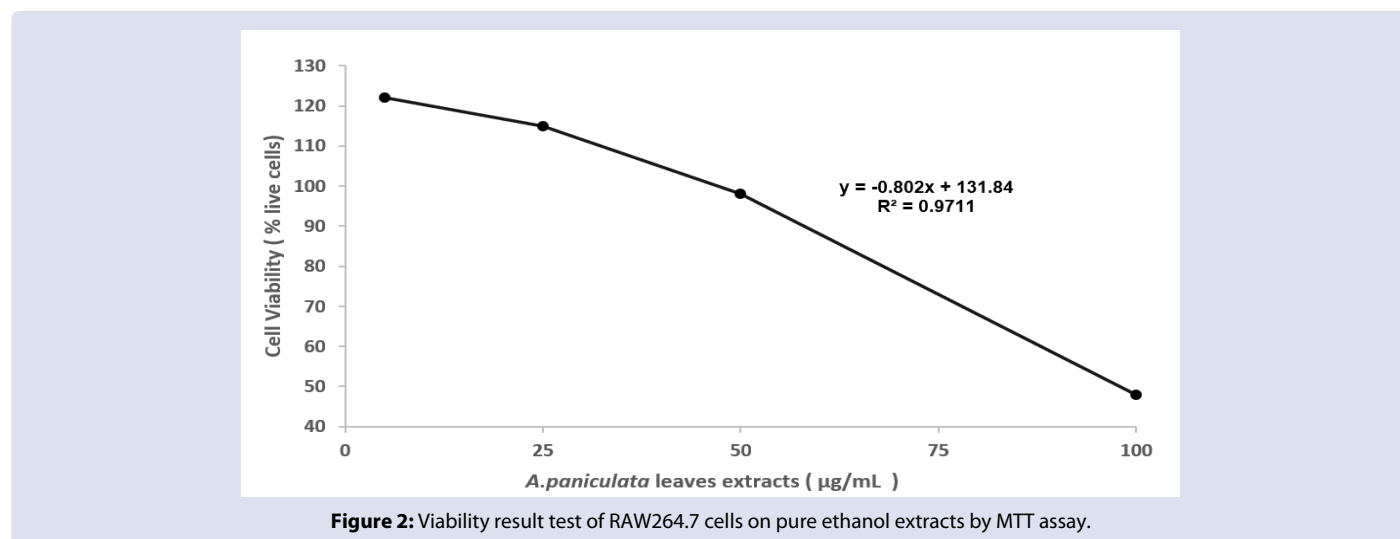


**Figure 2:** Viability result test of RAW264.7 cells on pure ethanol extracts by MTT assay.

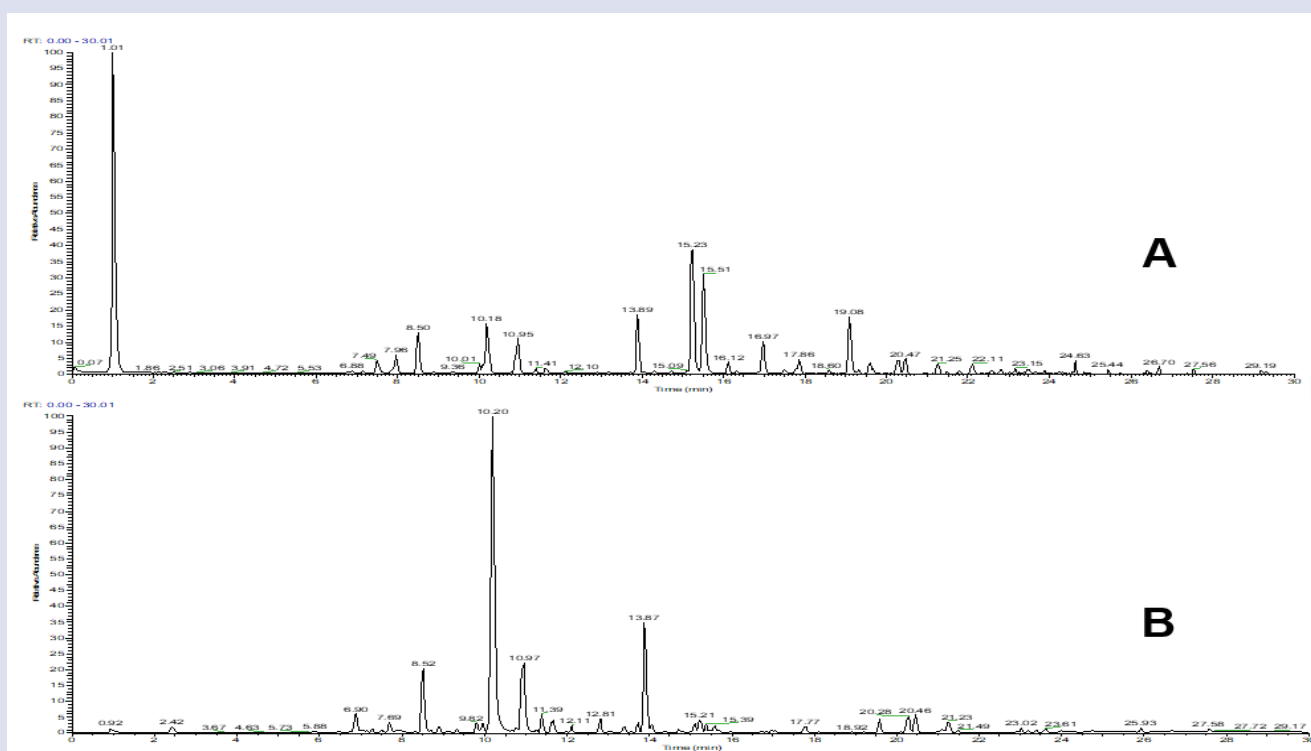


**Figure 3:** Representative chromatogram of pure ethanol extracts of *A. paniculata* leaves in positive ionization mode (A) and negative ionization mode (B).

**Table 5: Effect of *A. paniculata* extract on inhibition release of pro-inflammatory cytokines in RAW 264.7 cells.**

Samples	Cytokine Level (pg/mL ± SD)			Inhibition Activity over positive control (%)		
	TNF-α	IL-1β	IL-6	TNF-α	IL-1β	IL-6
Negative control (cells only)	7.040 ± 0.88	3.781 ± 0.714	2.085 ± 0.53	49.547 ± 4.93	71.871 ± 3.43	84.25 ± 3.49
Positive control (LPS alone)	13.971 ± 1.28	13.376 ± 1.22	13.175 ± 0.57	0.00 ± 0.00	0.00 ± 0.00	0.00 ± 0.00
LPS/extract (20 µg/mL)	0.000 ± 0.00	0.000 ± 0.00	6.401 ± 0.72	100.00 ± 0.00	100.00 ± 0.00	51.23 ± 7.17
LPS/extract (30µg/mL)	0.000 ± 0.00	0.000 ± 0.00	3.699 ± 0.91	100.00 ± 0.00	100.00 ± 0.00	71.75 ± 5.29
LPS/extract (40 µg/mL)	0.000 ± 0.00	0.000 ± 0.00	1.889 ± 0.40	100.00 ± 0.00	100.00 ± 0.00	85.59 ± 3.41

**Table 6: Putative identification of metabolites in pure ethanol extracts of *A. paniculata* leaves.**

No.	Name of Metabolites	RT [min]	Formula	MW	Error Mass (ppm)	Ion mode	MS-MS
1	14-Acetylandrographolide	15.16	C <sub>22</sub> H <sub>32</sub> O <sub>6</sub>	392.2199	-0.05	[M-H] <sup>-</sup>	391, 345, 301
2	14-Deoxy-11,12-didehydroandrographolide	10.11	C <sub>20</sub> H <sub>28</sub> O <sub>4</sub>	332.1978	-2.99	[M+H] <sup>+</sup>	333, 315, 297, 285, 257
3	14-Deoxy-11-oxo-andrographolide	10.17	C <sub>20</sub> H <sub>28</sub> O <sub>5</sub>	348.1927	-2.7	[M+H] <sup>+</sup>	349, 331, 313, 285
4	14-Deoxy-17-hydroxyandrographolide	7.76	C <sub>20</sub> H <sub>32</sub> O <sub>5</sub>	352.2238	-3.32	[M+H] <sup>+</sup>	353, 317, 299, 287
5	14-Deoxyandrographolide	15.28	C <sub>20</sub> H <sub>30</sub> O <sub>4</sub>	334.2132	-3.75	[M+H] <sup>+</sup>	335, 317, 299, 287, 259
6	14-Deoxyandrographoside	10.83	C <sub>26</sub> H <sub>40</sub> O <sub>9</sub>	496.2656	-3.34	[M+H] <sup>+</sup>	497, 299, 287, 259
7	3,14-Dideoxyandrographolide	13.92	C <sub>20</sub> H <sub>30</sub> O <sub>3</sub>	318.2183	-3.83	[M+H] <sup>+</sup>	319, 301, 289
8	5-Hydroxyjasmonic acid 5-O-hexoside	2.45	C <sub>19</sub> H <sub>30</sub> O <sub>8</sub>	386.1931	-2.47	[M+H] <sup>+</sup>	387, 351, 207, 149
9	5-Hydroxy-7,8-dimethoxyflavanone	21.01	C <sub>17</sub> H <sub>16</sub> O <sub>5</sub>	300.0986	-3.78	[M+H] <sup>+</sup>	301, 197
10	7-O-metilwogonin	21.97	C <sub>17</sub> H <sub>14</sub> O <sub>5</sub>	298.083	-3.65	[M+H] <sup>+</sup>	299, 285
11	Andrografolakton	15.57	C <sub>20</sub> H <sub>24</sub> O <sub>2</sub>	296.1768	-2.8	[M+H] <sup>+</sup>	297, 269, 255
12	Andrographic acid	6.58	C <sub>20</sub> H <sub>28</sub> O <sub>6</sub>	364.1879	-1.82	[M+H] <sup>+</sup>	365, 347, 329
13	Andrographiside	6.75	C <sub>26</sub> H <sub>40</sub> O <sub>10</sub>	512.2613	-1.63	[M+H] <sup>+</sup>	513, 351, 333, 315, 297, 285, 257
14	Andrographolide	7.58	C <sub>20</sub> H <sub>30</sub> O <sub>5</sub>	350.2082	-3.1	[M+H] <sup>+</sup>	351, 333, 315, 297, 285, 257
15	Apigenin-7-O-glucuronide	7.58	C <sub>21</sub> H <sub>18</sub> O <sub>11</sub>	446.0839	-2.36	[M+H] <sup>+</sup>	447, 271, 153
16	Bisandrographolide A	15.57	C <sub>40</sub> H <sub>56</sub> O <sub>8</sub>	664.396	-2.23	[M+H] <sup>+</sup>	665, 315, 297, 285
17	Diterpene II (Lactone)	10.28	C <sub>20</sub> H <sub>26</sub> O <sub>5</sub>	346.1769	-3.22	[M+H] <sup>+</sup>	347, 329, 283
18	Neoandrographolide	13.93	C <sub>26</sub> H <sub>40</sub> O <sub>8</sub>	480.2712	-2.3	[M+H] <sup>+</sup>	481, 319, 301, 289
19	Quinic acid	1.11	C <sub>7</sub> H <sub>12</sub> O <sub>6</sub>	192.0629	-2.68	[M-H] <sup>-</sup>	191, 147, 87, 85
20	Scoparin	8.37	C <sub>22</sub> H <sub>22</sub> O <sub>11</sub>	462.1155	-1.57	[M+H] <sup>+</sup>	463, 301, 287

LPS stimulation in positive controls can increase TNF- $\alpha$ , IL-1 $\beta$ , and IL-6 up to 84.25% when compared to negative controls. The inhibitory activity of pro-inflammatory cytokine production in macrophage cells treated with the extract showed very significant inhibitory potential.

At a test dose of 20 ppm, the extract was able to inhibit the production of pro-inflammatory cytokines TNF- $\alpha$  and IL-1 $\beta$  up to 100%, a different thing was shown in the inhibitory activity of pro-inflammatory cytokine IL-6 at test doses of up to 40 ppm it was able to inhibit up to 85.59 %.

Research on *A. paniculata* as an anti-inflammatory has been carried out, andrographolide, dehydroandrographolide, and neoandrographolide are the most widely reported metabolite compounds that have anti-inflammatory potential through various targets and pathways of inhibition.

Andrographolide is reported to suppress the production of pro-inflammatory cytokines such as TNF- $\alpha$ , IL-1 $\beta$ , IL-16, IL-12, and IL-18 in activated macrophages.<sup>38</sup> Andrographolide works by inhibiting the NF- $\kappa$ B activation pathway.<sup>39</sup> Kim et al. also reported that andrographolide inhibited pro-inflammatory cytokines by suppressing mitogen-activated protein kinase (MAPK) and activating the AMP-activated protein kinase (AMPK) pathway in LPS-induced macrophages.<sup>40</sup> Nareika et al. reported that andrographolide inhibited nitric oxide (NO) synthesis in LPS-stimulated RAW 264.7 cells by inhibiting protein synthesis inducible nitric oxide synthase (iNOS) so that NO production in cells decreased.<sup>41</sup> Several other studies have also reported that andrographolide interferes directly or indirectly with various targets involved in the inflammatory process such as inflammatory cytokines,<sup>4</sup> andrographolide inhibits cyclooxygenase-2 (COX-2),<sup>42</sup> inducible nitric oxide synthase,<sup>43</sup> and Interferon gamma (IFN- $\gamma$ ).<sup>44</sup> Andrographolide, dehydroandrographolide, and neoandrographolide are also reported to exhibit anti-inflammatory activity by inhibiting cyclooxygenase-1 (COX)-1, cyclooxygenase-2 (COX)-2, inhibiting the NF- $\kappa$ B activation pathway.<sup>45</sup>

In addition, the crude extract of *A. paniculata* showed strong inhibitory activity on pro-inflammatory mediators such as NO, IL-1 $\beta$ , and IL-6.<sup>46</sup> Several studies have also reported that andrographolide has anti-inflammatory activity in the lungs.<sup>47</sup> Li et al. reported that andrographolide *in vivo* tests on rats were shown to reduce allergen-induced inflammation, cellular infiltration in the airways, and airway hyperresponsiveness by inhibiting NF- $\kappa$ B expression in the lungs, in the nucleus and the airway epithelial cells.<sup>1</sup>

Various studies on the anti-inflammatory activity of *A. paniculata* metabolites can inhibit various types of targets and production pathways of pro-inflammatory mediators, and this condition is in line with the target of therapy in cases of COVID-19 infection. Inhibition of pro-inflammatory mediators in the early stages of COVID-19 infection is an effective therapeutic strategy to prevent the development of more severe ARDS.<sup>7</sup>

Pure ethanol extract of *A. paniculata* with the potential to inhibit the production of pro-inflammatory cytokines TNF- $\alpha$  and IL-1 $\beta$  by 100% and IL-6 inhibitory activity of up to 85.59% is a potential anti-inflammatory agent candidate for the treatment of inflammation-related diseases including COVID-19. It is necessary to characterize the metabolites of pure ethanol extract of *A. paniculata* leaves to determine the specific metabolites that have the potential as pro-inflammatory anti-cytokines.

## Identification of Metabolite Compounds

The metabolites of the ethanol extract of *A. paniculata* leaves were separated and identified using UHPLC-Q-Orbitrap HRMS to determine the composition of the extracted metabolites. The chromatogram in the positive ionization mode produces more metabolites when compared to the negative ionization mode (Figure 3).

A total of 20 metabolites were identified in the pure ethanol extract of *A. paniculata* leaves consisting of 4 metabolites belonging to the flavonoid class, 2 metabolites belonging to the phenolic acid group and 14 metabolites belonging to the diterpene lactone group (Table 6).

Andrographolide, dehydroandrographolide, and neoandrographolide are the most widely reported metabolites of *A. paniculata* with anti-inflammatory potential. However, other metabolites that play a more specific role in inhibiting the production of pro-inflammatory cytokines have not been widely reported. Compounds 14-Deoxyandrographoside and 14-Deoxy-17-hydroxyandrographolide are compounds of the diterpene lactone group, which are thought to have only been identified in ethanol extracts.

The 14-Deoxyandrographoside compound was identified in the positive ionization mode with a retention time of 10.83 and was fragmented at  $m/z$  497.27469 [M+H]<sup>+</sup>, 335.185 [M+H-Glc]<sup>+</sup>, 317.174 [M+H-Glc-2H<sub>2</sub>O]<sup>+</sup>, 299.164 [M+H-Glc-2H<sub>2</sub>O]<sup>+</sup> and 287.16382 [M+H-Glc-2H<sub>2</sub>O-C]<sup>+</sup>. The 14-Deoxy-17-hydroxyandrographolide compound was identified in the positive ionization mode with a retention time of 7.76 and was fragmented at  $m/z$  353.23282 [M+H]<sup>+</sup>, 335.22214 [M+H-H<sub>2</sub>O]<sup>+</sup>, 317.21164 [M+H-2H<sub>2</sub>O]<sup>+</sup>, 299.20032 [M+H-3H<sub>2</sub>O]<sup>+</sup> and 271.20468 [M+H-3H<sub>2</sub>O-CO]<sup>+</sup>. The potential of the compounds 14-Deoxyandrographoside and 14-Deoxy-17-hydroxyandrographolide as an anti-inflammatory has not been reported.

## CONCLUSIONS

Pure ethanol extract with specific metabolites 14-Deoxyandrographoside and 14-Deoxy-17-hydroxyandrographolide showed activity in inhibiting the production of pro-TNF- $\alpha$  and IL-1 $\beta$  cytokines by 100% and IL-6 by 85.59%. The *in silico* analysis and ADMET prediction for the metabolite compound 14-Deoxyandrographoside showed good binding stability of -7.5 kcal/mol to the CD14 receptor when compared to the Dexamethasone compound as a positive control of -7.44 kcal/mol. 14-Deoxyandrographoside is safe against several ADMET indicators. Ethanol extract of *A. paniculata* is a potential anti-inflammatory agent candidate for treating inflammation-related diseases, including COVID-19 infection.

## REFERENCES

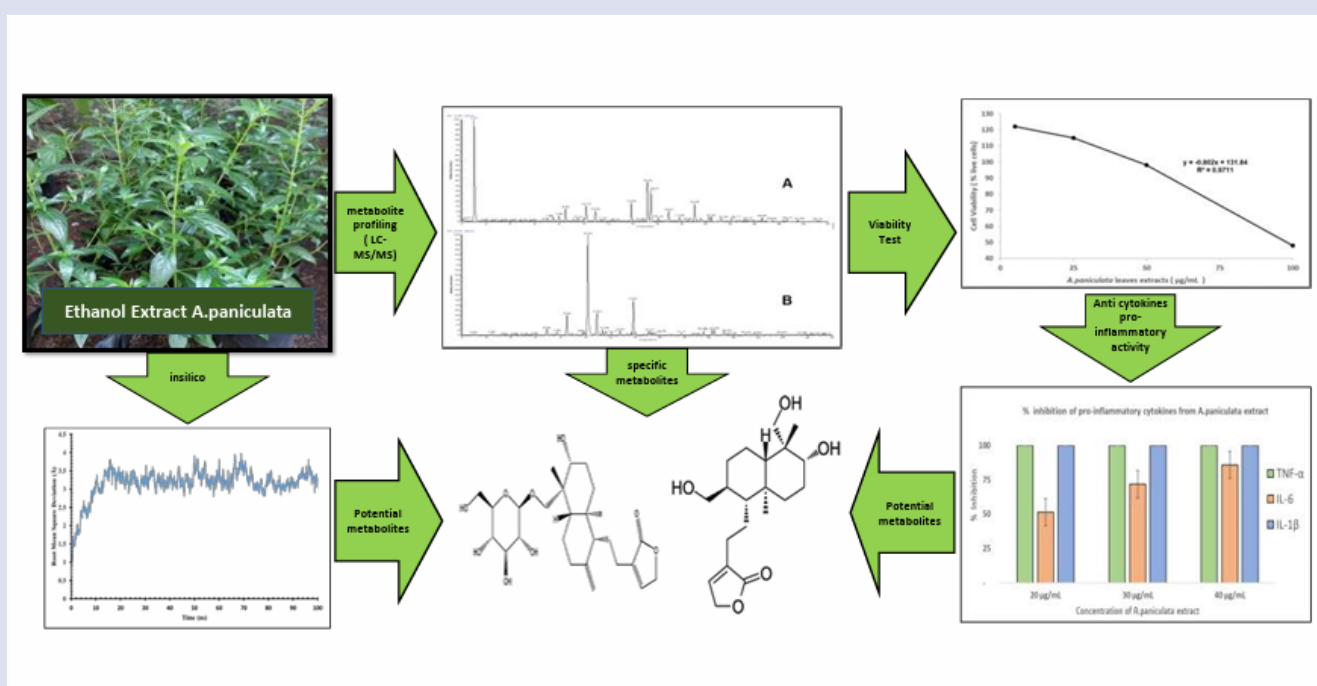
1. Li Q, Guan X, Wu P, et al. Early Transmission Dynamics in Wuhan, China, of Novel Coronavirus-Infected Pneumonia. *N Engl J Med*. 2020;382(13):1199-1207. doi:10.1056/nejmoa2001316
2. Woolf SH, Chapman DA, Sabo RT, Weinberger DM, Hill L, Taylor DSDH. Excess Deaths from COVID-19 and Other Causes, March-July 2020. *JAMA - J Am Med Assoc*. 2020;324(15):1562-1564. doi:10.1001/jama.2020.19545
3. Wu C, Chen X, Cai Y, et al. Risk Factors Associated with Acute Respiratory Distress Syndrome and Death in Patients with Coronavirus Disease 2019 Pneumonia in Wuhan, China. *JAMA Intern Med*. 2020;180(7):934-943. doi:10.1001/jamainternmed.2020.0994
4. Alzahrani A. A New Investigation into the Molecular Mechanism of Andrographolide towards Reducing Cytokine Storm. *Molecules*. 2022;27(14). doi:10.3390/molecules27144555
5. Tay MZ, Poh CM, Rénia L, MacAry PA, Ng LFP. The trinity of COVID-19: immunity, inflammation and intervention. *Nat Rev Immunol*. 2020;20(6):363-374. doi:10.1038/s41577-020-0311-8
6. Jose RJ, Manuel A. COVID-19 cytokine storm: the interplay between inflammation and coagulation. *Lancet Respir Med*. 2020;8(6):e46-e47. doi:10.1016/S2213-2600(20)30216-2
7. Wang J, Yang X, Li Y, Huang J an, Jiang J, Su N. Specific cytokines in the inflammatory cytokine storm of patients with COVID-19-associated acute respiratory distress syndrome and extrapulmonary multiple-organ dysfunction. *Viral J*. 2021;18(1):1-12. doi:10.1186/s12985-021-01588-y

8. Wasityastuti W, Dhamarjati A, Siswanto S. Immunosenescence and the Susceptibility of the Elderly to Coronavirus Disease 2019 (COVID-19). *J Respirologi Indones*. 2020;40(3):182-191. doi:10.36497/jri.v40i3.115
9. Rahminiwati M, Trivadila, Iswanti D, et al. Indonesian Medicinal Plants with Anti-inflammatory Properties and Potency as Chronic Obstructive Pulmonary Disease (COPD) Herbal Medicine. *Pharmacogn J*. 2022;14(4):432-444. doi:10.5530/pj.2022.14.119
10. Enmozhi SK, Raja K, Sebastine I, Joseph J. Andrographolide as a potential inhibitor of SARS-CoV-2 main protease: an in silico approach. *J Biomol Struct Dyn*. 2020;0(0):1-7. doi:10.1080/07391102.2020.1760136
11. Sukardiman, Ervina M, Pratama MRF, Poerwono H, Siswodihardjo S. The coronavirus disease 2019 main protease inhibitor from *Andrographis paniculata* (Burm.f) Ness. *J Adv Pharm Technol Res*. 2020;11(4):157-162. doi:10.4103/japtr.JAPTR\_84\_20
12. Sa-Ngiamsuntorn K, Suksatu A, Pewkliang Y, et al. Anti-SARS-CoV-2 Activity of *Andrographis paniculata* Extract and Its Major Component Andrographolide in Human Lung Epithelial Cells and Cytotoxicity Evaluation in Major Organ Cell Representatives. *J Nat Prod*. 2021;84(4):1261-1270. doi:10.1021/acs.jnatprod.0c01324
13. Hossain MS, Urbi Z, Sule A, Rahman KMH. *Andrographis paniculata* (Burm. f.) Wall. ex Nees: A review of ethnobotany, phytochemistry, and pharmacology. *Sci World J*. 2014;2014. doi:10.1155/2014/274905
14. Majumdar M, Singh V, Misra TK, Roy DN. In silico studies on structural inhibition of SARS-CoV-2 main protease Mpro by major secondary metabolites of *Andrographis paniculata* and *Cinchona officinalis*. *Biologia (Bratisl)*. 2022;77(5):1373-1389. doi:10.1007/s11756-022-01012-y
15. Intharuksa A, Arunotayanun W, Yoin W, Sirisa-ard P. A Comprehensive Review of *Andrographis paniculata* (Burm. f.) Nees and Its Constituents as Potential Lead Compounds for COVID-19 Drug Discovery. *Molecules*. 2022;27(14). doi:10.3390/molecules27144479
16. Dong ZB, Zhang YH, Zhao BJ, et al. Screening for anti-inflammatory components from *Corydalis bungeana* Turcz. based on macrophage binding combined with HPLC. *BMC Complement Altern Med*. 2015;15(1):1-10. doi:10.1186/s12906-015-0907-x
17. Hankittichai P, Buacheen P, Pitchakarn P, et al. *Artocarpus lakoocha* extract inhibits lps-induced inflammatory response in raw 264.7 macrophage cells. *Int J Mol Sci*. 2020;21(4). doi:10.3390/ijms21041355
18. Sujono TA, Kusumowati ITD, Munawaroh R. Aktivitas Imunomodulator Ekstrak Metanol dan Fraksi buah Talok (*Muntingia calabura* L.) pada Sel RAW 264.7. *JPSCR J Pharm Sci Clin Res*. 2021;6(2):82. doi:10.20961/jpscr.v6i2.47009
19. Jimenez-Duran G, Luque-Martin R, Patel M, et al. Pharmacological validation of targets regulating CD14 during macrophage differentiation. *EBioMedicine*. 2020;61. doi:10.1016/j.ebiom.2020.103039
20. Park SE, Yoo SA, Seo SH, Lee KI, Na CS, Son HS. GC-MS based metabolomics approach of Kimchi for the understanding of *Lactobacillus plantarum* fermentation characteristics. *Lwt*. 2016;68:313-321. doi:10.1016/j.lwt.2015.12.046
21. Wang Y, Jiao J, Yang Y, Yang M, Zheng Q. Screening and identification for immunological active components from *andrographis herba* using macrophage biospecific extraction coupled with UPLC/Q-TOF-MS. *Molecules*. 2018;23(5):1-11. doi:10.3390/molecules23051047
22. Neese F. Software update: the ORCA program system, version 4.0. *Wiley Interdiscip Rev Comput Mol Sci*. 2018;8(1):1-6. doi:10.1002/wcms.1327
23. Gani MA, Nurhan AD, Putri BRKH, et al. Computational approach in searching for dual action multitarget inhibitors for osteosarcoma. *J Adv Pharm Technol Res*. 2023;14(1):18-23. doi:10.4103/japtr.japtr\_541\_22
24. Gauthier T, Chen W. Modulation of Macrophage Immunometabolism: A New Approach to Fight Infections. *Front Immunol*. 2022;13(January):1-21. doi:10.3389/fimmu.2022.780839
25. Wakamiya R, Seki H, Ideno S, et al. Effects of prophylactic dexamethasone on postoperative nausea and vomiting in scoliosis correction surgery: a double-blind, randomized, placebo-controlled clinical trial. *Sci Rep*. 2019;9(1):1-7. doi:10.1038/s41598-019-38764-8
26. McHardy PG, Singer O, Awad IT, et al. Comparison of the effects of perineural or intravenous dexamethasone on low volume interscalene brachial plexus block: a randomised equivalence trial. *Br J Anaesth*. 2020;124(1):84-91. doi:10.1016/j.bja.2019.08.025
27. Darden T, York D, Pedersen L. Particle mesh Ewald: An N-log(N) method for Ewald sums in large systems. *J Chem Phys*. 1993;98(12):10089-10092. doi:10.1063/1.464397
28. Hardianto A, Muscifa ZS, Widayat W, Yusuf M, Subroto T. The Effect of Ethanol on Lipid Nanoparticle Stabilization from a Molecular Dynamics Simulation Perspective. *Molecules*. 2023;28(12). doi:10.3390/molecules28124836
29. Rafi M, Devi AF, Syafitri UD, et al. Classification of *Andrographis paniculata* extracts by solvent extraction using HPLC fingerprint and chemometric analysis. *BMC Res Notes*. 2020;13(1):1-6. doi:10.1186/s13104-020-4920-x
30. Fajriah S, Handayani S, Sinurat E, et al. In vitro Immunomodulatory Effect from Edible Green Seaweed of *Caulerpa lentillifera* Extracts on Nitric Oxide Production and Phagocytosis Activity of RAW 264.7 Murine Macrophage Cells. *J Young Pharm*. 2020;12(4):334-337. doi:10.5530/jyp.2020.12.87
31. Riss TL, Moravec RA, Niles AL, et al. Cell Viability Assays. *Assay Guid Man*. Published online 2004:1-31. <http://www.ncbi.nlm.nih.gov/pubmed/23805433>
32. Methods C aided DD. Antibiotics. *Biotechnol Bioeng*. 1965;7(1):29-51. doi:10.1002/bit.260070109
33. Syahputra G, Ambarsari L, T S. Simulasi docking kurkumin enol, bisdemetoksikurkumin dan analognya sebagai inhibitor enzim 12-lipoksigenase. *J Biofisika*. 2014;10(1):55-67.
34. Azzahra RW, Murdaya N, Al Shofwan AA, Ramadan E, Utami SD. Molecular Docking Senyawa Ekstrak Etanol Daun Kenikir (*Cosmos caudatus*) Sebagai Inhibitor Il-6 Dalam Respon Inflamasi. *J Farm Udayana*. 2021;10(2):138. doi:10.24843/jfu.2021.v10.i02.p05
35. Cheng F, Li W, Zhou Y, et al. AdmetSAR: A comprehensive source and free tool for assessment of chemical ADMET properties. *J Chem Inf Model*. 2012;52(11):3099-3105. doi:10.1021/ci300367a
36. Guan L, Yang H, Cai Y, et al. ADMET-score-a comprehensive scoring function for evaluation of chemical drug-likeness. *Medchemcomm*. 2019;10(1):148-157. doi:10.1039/C8MD00472B
37. Muniandy K, Gothai S, Badran KMH, Kumar SS, Esa NM, Arulselvan P. Suppression of proinflammatory cytokines and mediators in LPS-Induced RAW 264.7 macrophages by stem extract of *alternanthera sessilis* via the inhibition of the NF- $\kappa$ B pathway. *J Immunol Res*. 2018;2018. doi:10.1155/2018/3430684
38. Fox K, Ford I, Steg PG, Tardif JC, Tendera M, Ferrari R. Ivabradine in Stable Coronary Artery Disease without Clinical Heart Failure. *N Engl J Med*. 2014;371(12):1091-1099. doi:10.1056/nejmoa1406430
39. Cui J, Gao J, Li Y, et al. Andrographolide sulfate inhibited NF- $\kappa$ B activation and alleviated pneumonia induced by poly I:C in mice. *J Pharmacol Sci*. 2020;144(4):189-196. doi:10.1016/j.jphs.2020.08.005
40. Kim N, Lertnimitphun P, Jiang Y, et al. Andrographolide inhibits inflammatory responses in LPS-stimulated macrophages and murine acute colitis through activating AMPK. *Biochem Pharmacol*. 2019;170(September):113646. doi:10.1016/j.bcp.2019.113646
41. Nareika A, He L, Game BA, et al. Sodium lactate increases LPS-stimulated MMP and cytokine expression in U937 histiocytes by enhancing AP-1 and NF- $\kappa$ B transcriptional activities. *Am J Physiol - Endocrinol Metab*. 2005;289(4 52-4):534-543. doi:10.1152/ajpendo.00462.2004



42. Peng Y, Wang Y, Tang N, et al. Andrographolide inhibits breast cancer through suppressing COX-2 expression and angiogenesis via inactivation of p300 signaling and VEGF pathway 11 Medical and Health Sciences 1112 Oncology and Carcinogenesis. *J Exp Clin Cancer Res.* 2018;37(1):1-14.
43. Agarwala R, Barrett T, Beck J, et al. Database Resources of the National Center for Biotechnology Information. *Nucleic Acids Res.* 2017;45(D1):D12-D17. doi:10.1093/nar/gkw1071
44. Wurlina, Mustofa I, Meles DK, Utama S, Susilowati S. Immunostimulator Effect of Sambiloto (Andrographis paniculata L) Alkaloid in Rat (Rattus norvegicus). *Biotechnol Strengthen Biomed Sci Vet Med.* 2017;11(9):1-8. <https://www.bing.com/ck/a?!&p=0492948c2fef59cc6ab79d56d0033fedaa0ff21e1266ab26b9d0cbebc448e66aJmldtHM9MTY1NjQ1OTA0NCZpZ3VpZD1hMmE1NDhINC0wNWE1LTRjNWQtd0DMxMC1INjFIOTdINjRhOTUmaW5zaWQ9NTE0OQ&ptn=3&fclid=548c3339-f73a-11ec-b967-3cbdf2bf6f05&u=a1aHR0cHM6Ly93>
45. Nie X, Chen SR, Wang K, et al. Attenuation of Innate Immunity by Andrographolide Derivatives Through NF- $\kappa$ B Signaling Pathway. *Sci Rep.* 2017;7(1):1-10. doi:10.1038/s41598-017-04673-x
46. Lin HC, Li CC, Yang YC, et al. Andrographis paniculata diterpenoids and ethanolic extract inhibit TNF  $\alpha$ -induced ICAM-1 expression in EA.hy926 cells. *Phytomedicine.* 2019;52:157-167. doi:10.1016/j.phymed.2018.09.205
47. Dai Y, Chen SR, Chai L, Zhao J, Wang Y, Wang Y. Overview of pharmacological activities of andrographis paniculata and its major compound andrographolide. *Crit Rev Food Sci Nutr.* 2019;59(0):S17-S29. doi:10.1080/10408398.2018.1501657

## GRAPHICAL ABSTRACT



## ABOUT AUTHORS



**Evul Winoto Lukio** is a doctoral student in chemistry, Faculty of Mathematics and Natural Sciences at the Graduate School of IPB University, Indonesia. He is working as head of research and development at the Biomedical Institute Puskesad, Jakarta.



**Dyah Iswantini** is a Professor at the Department of Chemistry, Faculty of Mathematics and Natural Sciences, IPB University, Indonesia. She is an expert on secondary metabolites for anti-obesity, antigout, anti-inflammatory, and antihypertension from kinetics and thermodynamic point of view.



**Dr. Budhi Antariksa, Ph.D., Sp.P(K)** is a renowned pulmonologist and respiratory medicine specialist in Indonesia. He holds degrees from University of Indonesia and Hiroshima University and is a Specialist in the Lung and Breathing Field, focused on Asthma and COPD. His career also includes leadership roles at Persahabatan Hospital, University of Indonesia, and The Indonesia Society of Respirology Jakarta Branch. He has published over 50 articles in national and international journals and authored 14 books. His work in various symposiums, seminars, and conferences has established him as a leading voice in his field.



**Mohamad Rafi** is a Professor in Analytical Separation at the Department of Chemistry and Natural Sciences, IPB University, Indonesia. His expertise is on Analytical Separation, Analytical Spectroscopy, Chemometrics and Metabolomics. His research focus in the method development of medicinal plants quality control and application metabolomics in natural products research. He has published more than 150 scientific articles in national and international journals.



**Setyanto Tri Wahyudi** is an assistant Professor at Department of Physics, Faculty of Mathematics and Natural Sciences, IPB University, Indonesia. He is an expert on molecular modelling, docking and molecular dynamics simulation. His research mainly on Malaria and TBC drug target, Thermostability Lipase and other Industrial in enzyme in computational point of view.

**Cite this article:** Lukito EW, Iswantini D, Antariksa B, Rafi M, Wahyudi ST. Screening and Identification of Metabolites from Sambiloto (*Andrographis paniculata*) Ethanol Extract for Pro-Inflammatory Cytokines Inhibitory through *In Silico* and *In Vitro* Approaches. *Pharmacogn J.* 2024;16(1): 131-140.